J. Plasma Fusion Res. SERIES, Vol. 5 (2002) 288–291

# Recent Experiments in Heliotron J

OBIKI Tokuhiro, SANO Fumimichi, KONDO Katsumi[1], WAKATANI Masahiro[1], MIZUUCHI Tohru, HANATANI Kiyoshi, NAKAMURA Yuji[1], NAGASAKI Kazunobu, OKADA Hiroyuki, BESSHOU Sakae[1], NAKASUGA Masahiko[1], TSURU Hiroki[1], MANABE Yoshito[1], SHIDARA Hiroyuki[1], ANG Wanleng[1], TAKAMIYA Tasho[1], IRIGUCHI Masao[1], TAKEDA Masafumi[1], KAWAZOME Hayato[1], MAENO Shogo[1], TOMIYAMA Keishi[1], OHNO Yoshinori[1], KUBO Hiroyasu[1], NISHIOKA Yusuke[1], YUKIMOTO Hidetoshi[1], IJIRI Yoshiyuki, SENJU Tohru, YAGUCHI Keiji, SAKAMOTO Kinzou, TOHSHI Kiyoshi, SHIBANO Masashi, TABARÉS Francisco[2] and TRIBALDOS Victor[2]

*Institute of Advanced Energy, Kyoto University, Uji 611-0011, Japan*

*[1]Graduate School of Energy Science, Kyoto University, Uji 611-0011 , Japan*

*[2]Laboratorio Nacional de Fusión, Asociación EURATOM-CIEMAT, Madrid, Spain*

(Received: 21 December 2001 / Accepted: 4 June 2002)

## Abstract

Recent experiments in Heliotron J are reported with special regard to the ECH plasma confinement. After the initial verification of its sound magnetic surfaces, the 53.2 GHz, 400 kW ECH experiments in Heliotron J were carried out, leading to a successful production of the collisionless hydrogen plasmas with electron temperatures up to ~ 1 keV at low electron densities of $(0.2 - 0.3) \times 10^{19}$ m$^{-3}$ which allows us to study the characteristics of the $1/\nu$ electron transport in the helical-axis heliotron line. It was observed that the core confinement properties were strongly dependent on the selected plasma configuration, suggesting a possible link to the surface quantities such as its iota profile. In addition to the core properties, the edge and scrape-off-layer (SOL) plasma behavior is discussed, and also the initial results from the newly-installed 70-GHz ECH are presented.

## Keywords:

Heliotron J, heliotron, helical-axis heliotron, bumpiness, magnetic well, helical and island divertors

## 1. Introduction

In order to prepare the next generation of the heliotron line in the helical magnetic field configuration, Heliotron J was constructed with the aim of obtaining the experimental basis for the physics design principles in the "helical-axis heliotron". The main characteristics of Heliotron J are the strongly modulated helical variation of its magnetic axis, the resultant reduction of the neoclassical $1/\nu$ transport, the favorable MHD characteristics with its edge magnetic well and the operational capability of studying the island divertor as well as the helical divertor [1]. The magnetic field ($B \leq$ 1.5 T) is generated by the coil system of the $L = 1/M = 4$ helical conductor, two kinds of the toroidal coils and three kinds of vertical coils, as shown in Fig. 1 [2]. The iota value varies as its coil parameters in the range of 0.3 to 0.8 with a low magnetic shear under conditions when the major plasma radius of the plasma ($R$) is 1.2 m and the average minor radius of the plasma ($a_p$) is 0.1 – 0.2 m. As for the plasma heating systems, ECH (0.5 MW), NBI (1.5 MW) and ICRF (2 MW) are in preparation.

This paper discusses the recent results from the 53.2 GHz and 70 GHz ECH experiments in order to get an overview of the operational flexibility and the global

*Corresponding author's e-mail: obiki@iae.kyoto-u.ac.jp*

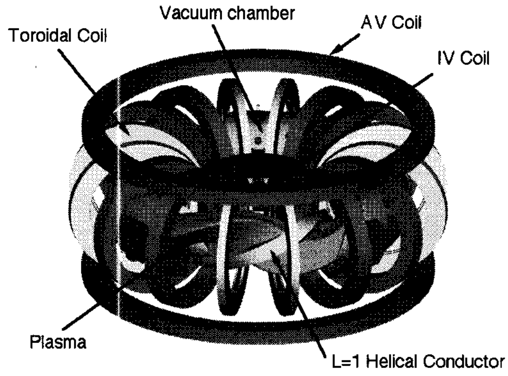


Fig. 1 Coil system of Heliotron J : $L = 1/M = 4$ helical conductor, two kinds of toroidal coils and three kinds of vertical coils (AV, IV, and V). The main vertical coil (V) is not seen in this figure.

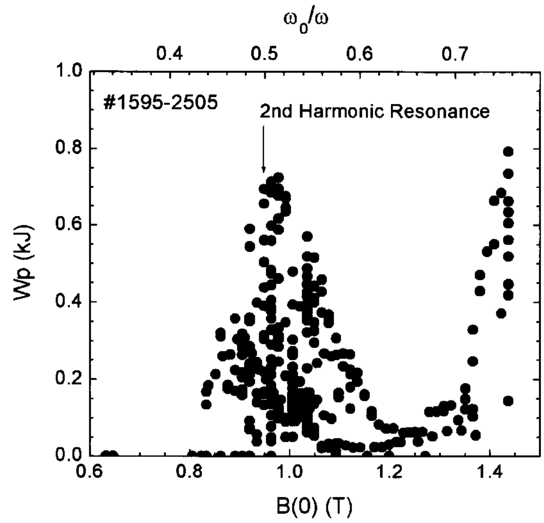


Fig. 2 Plasma internal energy $W_p$ as a function of the magnetic field $B(0)$ on the axis in the straight section under the condition of the 53.2 GHz, 400 kW ECH for the STD configuration.

confinement performance of Heliotron J before the detailed transport analysis that will be carried out from now on.

## 2. Electron Beam Mapping

Heliotron J is a flexible, concept-exploration-level facility to search for the optimized helical-axis heliotron from the experimental viewpoints. As such a device, the electron beam mapping study is essential to afford a foundation for its plasma confinement studies. Before entering into the plasma experiment, the mapping experiments at low magnetic fields (300 G) were made to confirm the existence of the closed and nested magnetic surfaces for the basic (BSC) and standard (STD) configurations, showing that the measured data were in fundamental agreement with the field line tracing calculations taking into account the earth magnetic field and the ambient magnetic field near the torus. See ref. [2]. With regard to the configuration effects around the BSC configuration that will be discussed below, the mapping experiments were also made as a function of the auxiliary vertical field coil current, $I_{AV}$. The results at low fields revealed the island formation and the shrinkage of the confinement region due to the emergence of low-order rational surface such as $\iota/2\pi = 1/2$ (or 4/7), but the influence of this error field (including the effect of the natural islands) on the plasma confinement at higher fields still needs the high-field mapping results to elucidate its origin.

## 3. ECH Plasma Production and Heating

After the experimental verification of the sound BSC and STD magnetic flux surfaces, ECH plasma production and heating studies were carried out using three 53.2 GHz gyrotrons. Two oblique injection launchers were located at the corner section of $\phi \sim 129°$ and one perpendicular injection launcher was located at the straight section of $\phi \sim 203°$, where $\phi$ is the toroidal angle starting from the middle position of the straight section selected as the origin. These microwaves of the $TE_{02}$ mode were injected from the outside of the torus through smoothed oversized waveguides. The total injection power was about 400 kW and the pulse width was 40–50 ms. As shown in Fig. 2, the optimal ECH heating was found to be in general agreement with that situation where the 2nd harmonic resonance layer could locate in the straight section of the confinement torus at $B(0) = 0.95$ T. In addition, the highly efficient ECH was also found to exist in the higher magnetic field region of more than $B(0) = 1.4$ T, where no resonance layer exists in the plasma core region. The fundamental resonance layer was located only at the edge region ($r/a_p \geq 0.8$) in a limited toroidal zone near the corner section, where the mod-B structure is tokamak-like and the magnetic field gradient is large. This heating mechanism remains to be studied in relation to the strong inward heat pinch or the electron Bernstein wave heating that was mode-converted from the edge fundamental ECH.

At low electron densities of $\bar{n}_e = (0.2 - 0.3) \times 10^{19}$ $m^{-3}$, the electron temperatures were measured by the soft X-ray absorber foil method to be ~ 1 keV, indicating the production of the collisionless plasmas of $\nu^* \ll 0.1$ in

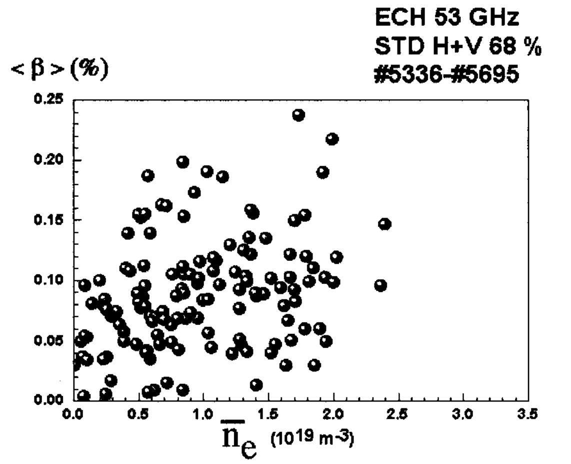


Fig. 3 Volume averaged beta $<\beta>$ as a function of line-averaged electron density $\bar{n}_e$ under the condition of the 53.2 GHz, 400 kW ECH at $B(0)$ = 0.95 T for the STD configuration.

their core regions, where $v^* = \pi R_0 q/(v_e \tau_e)$ and $v^* = 1$ stands for the normalized plateau collisionality. According to the DKES-code calculation [3], the neoclassical diffusion coefficient $D$ in this collisionless regime is expected to become comparable to that of the equivalent tokamak without the help of the electric field. Thus, these plasmas are expected to provide good opportunities to experimentally study the beneficial effect of the bumpiness on the collisionless electron transport in the helical-axis heliotron. On the other hand, at higher densities of $\bar{n}_e > 1.0 \times 10^{19}$ m$^{-3}$, the increase in internal plasma energy was observed. The diamagnetic measurement showed the maximum attainable internal energy $W_p \sim 0.7$ kJ or $<\beta> \sim 0.2$ % at $\bar{n}_e \sim 1.8 \times 10^{19}$ m$^{-3}$ which is near the cutoff density at $B(0)$ = 0.95 T for 53.2 GHz ECH, as shown in Fig. 3. Recently, a 70 GHz, 400 kW well-focused 2nd harmonic ECH experiment has been started, which has provided a plasma of $<\beta> \sim$ 0.3 % at $B$ = 1.25 T.

## 4. Configuration Effects

Magnetic configuration effects of Heliotron J were studied with special regard to the magnetic surface quantities by changing the coil current such as the auxiliary vertical coil current ($I_{AV}$) under conditions where the electron density was controlled with hydrogen gas puff. Because the change of $I_{AV}$ shifts the average minor radius of the confined plasma as well as the average major radius of the magnetic axis ($<R_{axis}>$), the iota ($\iota/2\pi$), etc. with reference to those of the basic configuration (BSC) in this experimental scan as shown

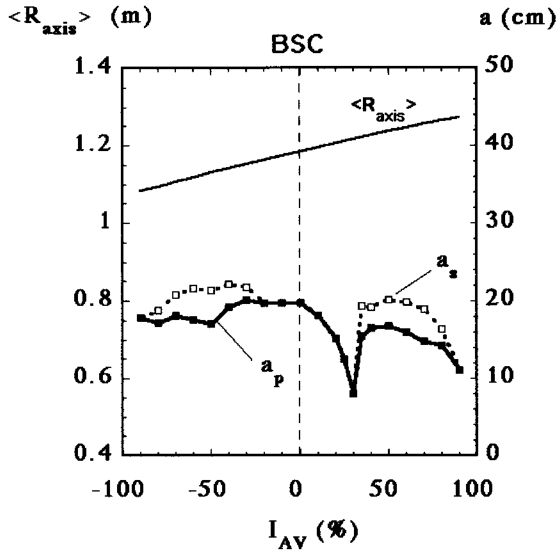


Fig. 4 Average minor radius of the confined plasma ($a_p$), average minor radius of the last closed magnetic surface without the vacuum chamber ($a_s$), and the average major radius of the magnetic axis $<R_{axis}>$ around the BSC configuration as a function of auxiliary vertical coil current $I_{AV}$. Under the condition of $a_p < a_s$, the confinement region is restricted by the chamber wall. Under the condition of $a_p = a_s$, it is determined by a magnetic separatrix. The setting of $I_{AV}$(100%) corresponds to $I_{AV}$ = 144 kAT.

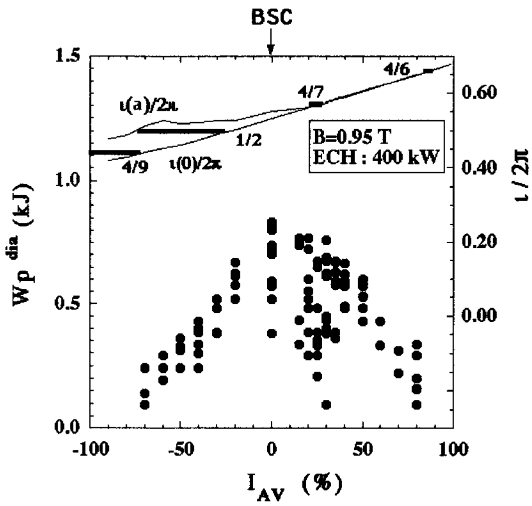


Fig. 5 Diamagnetic internal energy $W_p^{dia}$ as a function of the auxiliary vertical coil current $I_{AV}$ under the condition of 53.2 GHz, 400 kW ECH at $B(0)$ = 0.95 T. $\iota(a_p)/2\pi$ and $\iota(0)/2\pi$ show the central rotational transform and the edge rotational transform, respectively.

in Figs. 4 and 5, the magnetic field strength $B(0)$ on the axis was maintained to be 0.95 T (2nd harmonic resonance field) in order to attain the central 53.2 GHz, 400 kW ECH heating. As shown in Fig. 5, the experiment revealed that (i) the configurations of the outward axis shift ($\iota/2\pi > 0.53$) introduced a gradual decrease in the attainable plasma energy content, (ii) the configurations of the inward shift ($\iota/2\pi < 0.53$) introduced a rapid decrease in the energy content, and that (iii) the maximum energy content 0.7 kJ in this scan was obtained at the BSC ($\iota/2\pi = 0.53$). These results also revealed that the decrease in $W_p/a_p^2$ (the plasma energy content normalized with the corresponding confinement volume) at $\iota(0)/2\pi < 0.53$ was more marked than that of $\iota(0)/2\pi > 0.53$. Physics interpretations of these results should be made on the basis of the confinement dependences not only on the particle orbits in relation to the axis shift, but also on the key surface quantities such as the iota, magnetic shear, magnetic well, etc. From this viewpoint, the finding that both the energy content and the normalized energy content decreased under conditions when the low-order rational surface such as $\iota/2\pi = 1/2$ was introduced in the confinement region raised an important question as to the experimental soundness of the magnetic surface at the rational $\iota/2\pi$ value. With regard to the shift of the iota value, the plasma current effect is also a future issue to be measured and studied. In addition, the plasma-wall interactions should be clarified under the axis-shift conditions since the axis shift can easily cause a partial contact of the confining plasma with the stainless steel wall of Heliotron J. Thus, further experiments are needed to clear up these questions, but it was found that the initial plasmas in Heliotron J addressed a sensitive energy content dependence on the selected magnetic configuration, then encouraging future expectations to get experimental insights into its optimization.

## 5. Edge and SOL Properties

The detailed study of the edge and SOL properties is important to investigate the improvement of the core confinement as well as to study the divertor scenario in Heliotron J. The edge and SOL properties for ECH plasmas were measured using stationary or movable electro-static probes, and the typical parameters near the last closed surface in the SOL region were $T_e = 40 - 50$ eV and $n_e = 0.1 - 0.2 \times 10^{19}$ m$^{-3}$. The charged particle fluxes in the divertor region were also measured, and the result of the poloidal and toroidal distribution of the ion saturation current was found to be in basic agreement with the expectations from the calculated divertor footprints. In Heliotron J, a part of the whisker-field lines outside the confinement region in the STD (or BSC) configuration crosses the inner vacuum chamber wall, thus forming the divertor legs attached to the wall. The divertor legs have localized distributions on the wall with the dependence on the tracing direction. It was found that a strong up-down asymmetry was present in the profiles of density and floating potential on the geometrically symmetric upper and lower divertor legs. This asymmetry was reversed as the main magnetic field of the device was reversed. A possible explanation is that this asymmetry is due to the grad-$B$ drift [4].

## 6. Summary

The recent plasma experiments in Heliotron J have presented the following results:

For the BSC/STD configurations,

(1) the low-field mapping data were in basic agreement with the expectations,

(2) it was found that 53.2 GHz and 70 GHz 2nd harmonic ECH could provide collisionless plasmas in the core region, thus allowing us to examine the detailed $1/\nu$ electron transport in the helical-axis heliotron. The core electron temperature reached ~ 1 keV at low densities of $(0.2 - 0.3) \times 10^{19}$ m$^{-3}$. The diamagnetic $\langle\beta\rangle$ reached about 0.3 % for 70-GHz ECH,

(3) the obvious configuration effects of plasma confinement were observed in relation to the variation of the surface quantities such as the iota, but their definite interpretation still needs more experimental information such as the mapping data at high fields,

(4) the experimental understanding of the edge and SOL region is increasing.

## References


[1] F. Sano *et al.*, J. Plasma Fusion Res. SERIES **3**, 26 (2000).

[2] T. Obiki *et al.*, Nucl. Fusion **41**, 833 (2001).

[3] M. Wakatani *et al.*, Nucl. Fusion **40**,569 (2000).

[4] W. ANG *et al.*, *in this conference.*